Activation of the Non-receptor Tyrosine Kinase cSrc in Macrophage-rich Atherosclerotic Plaques of Human Carotid Arteries

Sono Toi[1], Noriyuki Shibata[2], Tatsuo Sawada[2], Makio Kobayashi[2] and Shinichiro Uchiyama[1]

[1]Department of Neurology, Tokyo Women's Medical University, 8–1 Kawada-cho, Shinjuku-ku, Tokyo 162–8666, Japan and
[2]Department of Pathology, Tokyo Women's Medical University, 8–1 Kawada-cho, Shinjuku-ku, Tokyo 162–8666, Japan

To determine the involvement of the non-receptor tyrosine kinase cSrc in plaque destabilization in carotid atherosclerosis (CAS), which is responsible for cerebral infarction, we performed quantitative and morphological detection of phosphorylated active cSrc (p-cSrc) and histopathological examination in CAS lesions. We examined carotid endarterectomy specimens obtained from 32 CAS patients. Each specimen was used for immunoblot and immunohistochemical analyses of p-cSrc, histopathological analysis, and image analysis of macrophage content. There was a strong positive correlation between cSrc activation on blots and macrophage content on sections. When we defined the macrophage-rich plaque (MRP) and the macrophage-poor plaque (MPP) as having macrophage content more and less than 5%, respectively, the p-cSrc density and the occurrence of plaque hemorrhage and thrombus formation were significantly increased in the MRP group (n=18) compared to the MPP group (n=14). p-cSrc immunoreactivity was localized in lesional endothelial cells, macrophages, and smooth muscle cells, which contained proinflammatory substances: the upstream oxidized low density lipoprotein, tissue factor and osteopontin, and the downstream active forms of extracellular signal-activated kinase and p38 and nuclear factor-κB. Our results suggest that cSrc activation in lesional cells contributes to plaque destabilization in CAS via persistent inflammation.

Key words: atherosclerosis, carotid artery, Src, inflammation, plaque instability

I.   Introduction

Several investigations have indicated that carotid atherosclerosis (CAS) is a major cause of cerebral infarction [1]. Acute-onset ischemic brain attack occurring in CAS patients results from acute occlusion of the lumen by atherothrombosis or hemorrhage in the plaques or from thromboembolism originating in atherothrombotic lesions [36, 37]. These events associated with CAS appear to be based on plaque instability, as described in studies on coronary atherosclerosis [11]. Emerging evidence suggests implications for persistent inflammation in plaque destabilization of carotid arteries [32]. Several studies on atherosclerosis of carotid and coronary arteries have shown that plaques containing a lot of macrophages are unstable, while those containing only a few macrophages are stable [11, 24, 32, 36, 37].

It has been shown that vascular endothelial cells (VECs), T-lymphocytes, and vascular smooth muscle cells (VSMCs) as well as macrophages participate in atherogenic inflammation [24, 32, 37]. VECs exposed to pathological conditions including risk factors for atherosclerosis release chemokines into blood and express cell adhesion molecules (CAMs) on the apical cell surface. Chemokines stimulate circulating monocytes to express integrin $\alpha_M\beta_2$ as the receptor for CAMs, and the binding of CAMs to integrin $\alpha_M\beta_2$ induces monocyte transmigration into the subendothelial vascular wall tissue. Migrating monocytes are transformed to macrophages in the presence of monocyte colony-

Correspondence to: Sono Toi, Department of Neurology, Tokyo Women's Medical University, 8–1 Kawada-cho, Shinjuku-ku, Tokyo 162–8666, Japan. E-mail: stoi@nij.twmu.ac.jp

stimulating factor released from T-lymphocytes. In atherosclerotic plaques, migrating VSMCs secrete collagen to form neointima, while macrophages secrete matrix metalloproteinases to degrade the surrounding extracellular collagen matrix. The latter leads to plaque destabilization, as evidenced by the vulnerability of the fibrous cap, followed by ulceration, hemorrhage, rupture, and thrombus formation, or both. Macrophages also secrete vascular endothelial growth factor, resulting in neovascularization in the plaques. The newly formed capillary vessels are mechanically vulnerable and readily rupture to form hematoma in the plaques, so-called plaque hemorrhage. All plaque-composing cells also secrete several cytokines and growth factors. These observations would indicate the crosstalk between the lesional cells in atherosclerotic plaques, and suggest that macrophage content is a marker of inflammation and destabilization of atherosclerotic plaques.

In atherogenesis, angiotensin II, oxidized low density lipoprotein (OxLDL), activated factor VII (FVIIa), and osteopontin have been shown to trigger inflammatory response, by binding to their receptors: angiotensin II type 1 receptor (AT_1R), scavenger receptor, tissue factor, and integrin $\alpha_v\beta_3$, CD44 or fibronectin, respectively [3, 8, 21, 24, 26, 27, 35, 38]. Actually, recent *in vivo* studies have shown increased levels of OxLDL, tissue factor, and osteopontin in macrophage-rich or symptomatic plaques [10, 14, 23]. Moreover, atherothrombosis is enhanced in animals overexpressing tissue factor [12] and osteopontin [6], while it is attenuated in animals deficient in tissue factor [34] and osteopontin [33]. These observations suggest critical roles for tissue factor and osteopontin in atherogenesis. Several *in vitro* studies have demonstrated that extracellular stimuli induced by angiotensin II, OxLDL, tissue factor, and osteopontin activate the non-receptor tyrosine kinase cSrc, collectively. cSrc is a proto-oncogene product that was identified as an intracellular homologue of the Rous sarcoma virus oncogene product vSrc [35]. cSrc is a 60 kDa protein, expressed ubiquitously in several types of cells including inflammatory cells, and localized in the cytosol under physiological conditions. The binding of extracellular ligands, such as growth factors, cytokines, factor VIIa, and osteopontin, to their respective membrane-bound receptors results in recruitment of the cytosolic cSrc to the intracellular domains of the receptors followed by phosphorylation-mediated activation of cSrc. The activated cSrc starts inflammatory and proliferative cell signaling via activation of mitogen-activated protein kinases (MAPKs) such as extracellular signal-regulated kinase (ERK), c-Jun N-terminal kinase (JNK), and p38 as well as transcription factors including nuclear factor-κB (NF-κB) [3–5, 7, 15, 21, 35]. However, it remains to be determined whether cSrc activation may occur in association with atherogenic inflammation and plaque destabilization *in vivo*. To address this issue, we investigated morphological and quantitative analyses of active form of cSrc phosphorylated at amino acid residue Y^{416} (p-cSrc) and verified the correlation between macrophage content and cSrc activation in CAS lesions. This is the first report concerning both immunohistochemical detection and quantitative measurement of p-cSrc in atherosclerotic plaques of human carotid arteries.

II. Materials and Methods

Subjects and tissue preparation

This study was approved by the Ethics Committee of Tokyo Women's Medical University and was carried out on 32 CAS patients [ages: 50–82 (69.7±8.2) y] who underwent carotid endarterectomy (CEA). The clinical features of the examined cases are summarized in Table 1. Each CEA specimen was divided into equal two parts and processed for making freshly frozen materials and 30% sucrose-immersed, optical cutting temperature (OCT) compound-embedded frozen materials. Both of them were stored at −80°C until use.

Immunoblot analysis

The primary antibodies employed in immunoblotting were mouse monoclonal IgG_1 against p-cSrc (Clone 9A6, Upstate, Lake Placid, NY, USA; 1:5,000) and mouse monoclonal IgG_1 against β-actin (Clone AC-15, Sigma, St. Louis, MO, USA; 1:10,000). Freshly frozen materials were homogenized with 10-fold volumes of radioimmunoprecipitation assay (RIPA) buffer consisting of 50 mM Tris-buffered saline, pH 7.5 (TBS), 1% sodium dodecyl sulfate (SDS), 1% glycerol, 1% deoxycholic acid, 0.1% Tween-20, and 0.3% 1,4-dithiothreitol (DTT) as well as the protease inhibitor cocktail Complete Mini® (Roche Diagnostics, Mannheim, Germany) according to the manufacturer's instructions. Ho-

Table 1. *Clinical features of examined cases*

Characteristics	n	%
Total number of subjects	32	100
Sex		
Male	28	87.5
Female	4	12.5
Phenotype		
Symptomatic case	12	37.5
Asymptomatic case	20	62.5
Risk factor		
Hypertension	24	75
Hyperlipidemia	14	43.8
Diabetes mellitus	10	31.3
Smoking	10	31.3
Ischemic heart disease	13	40.6
Therapeutic drugs		
Aspirin	28	87.5
Statin	9	28.1
Fibrate	0	0
TZD	0	0
ACEI	4	12.5
ARB	13	40.6

ACEI, angiotensin II-converting enzyme inhibitor; ARB, angiotensin II receptor blocker; TZD, thiazolidinedione.

mogenates were centrifuged for 15 min at 4°C with 15,000 g to obtain supernatant samples. Protein concentration of each sample was measured by the Bradford method [29], and samples were subsequently mixed with equal volume of Laemmli's buffer and boiled for 5 min. Aliquots of total protein extracts (30 μg/lane) were loaded on a 10% SDS-polyacrylamide gel, electrophoresed, and transferred onto a polyvinylidene difluoride (PVDF) membrane (Millipore, Tokyo, Japan). Blots were pretreated overnight at room temperature with 5% bovine serum albumin (BSA) in TBS containing 0.1% Tween-20 (TBS-T) solution, and then incubated with the anti-p-cSrc antibody in Can Get Signal® solution (Toyobo, Tokyo, Japan) for 1 hr at room temperature followed by horseradish peroxidase (HRP)-labeled anti-mouse IgG antibody (DakoCytomation, Kyoto, Japan; 1:10,000) in Can Get Signal® solution for 1 hr at room temperature. Immunoreaction for p-cSrc was visualized by the chemiluminescence method using the ECL-plus kit (GE Healthcare, Buckinghamshire, UK). Blots were then treated for 30 min at 50°C with a stripping buffer composed of 50 mM TBS, 2% SDS, and 1% β-mercaptoethanol, rinsed in TBS-T, treated overnight at room temperature with 5% skim milk/TBS-T solution, and incubated with the anti-β-actin antibody in 5% skim milk/TBS-T solution followed by the HRP-labeled anti-mouse IgG antibody in 5% skim milk/TBS-T solution. Immunoreaction for β-actin was detected with the ECL kit (GE). Lanes processed with omission of the primary antibodies or by incubating with nonimmune mouse IgG served as negative reaction controls. Immunoreactive signals for both p-cSrc and β-actin were developed on an X-ray film, imported into a personal computer using Photoshop image software, and quantitatively measured using CS analyzer (ATTO, Tokyo, Japan). Optical density of p-cSrc was normalized with that of β-actin in each lane. The densitometric p-cSrc/β-actin data were used for statistical analysis.

Histopathological analysis

Plaque morphology was histopathologically evaluated on sections stained with hematoxylin-eosin (H&E), focusing on the hallmarks of plaque instability such as ulceration, hemorrhage, thrombus formation, and calcification. The occurrence of these changes was statistically compared between the examined plaques.

Immunohistochemical analysis

The primary antibodies employed in immunohistochemistry were mouse monoclonal IgG$_1$ against p-cSrc (Clone 9A6; Upstate; 1:1,000), mouse monoclonal IgG$_1$ against CD68 (Clone KP-1; DakoCytomation; 1:10,000), mouse monoclonal IgG$_1$ against α-smooth muscle actin (SMA) (Clone 1A4; DakoCytomation; 1:1,000), mouse monoclonal IgM against oxidized phosphatidylcholine (OxPC) [13] (Clone DLH3; 1:3,000), mouse monoclonal IgG$_1$ against tissue factor (Clone 4509; American Diagnostica Inc., Stamford, CT, USA; 1:200), mouse monoclonal IgG$_1$ against osteopontin (Clone sc-21742; Santa Cruz Bio-

technology, Santa Cruz, CA, USA; 1:1,000), mouse monoclonal IgG$_{2a}$ against active form of ERK phosphorylated at Y^{204} (p-ERK) (Clone sc-7383; Santa Cruz; 1:200), rabbit polyclonal IgG against active form of p38 phosphorylated at Y^{182} (p-p38) (Cat. No. sc-7975-R; Santa Cruz; 1:200), and goat polyclonal IgG against NF-κB (Cat. No. sc-109-G; Santa Cruz; 1:200). CD68, SMA, and OxPC were used as markers of macrophage, VSMC, and OxLDL, respectively. Tissue factor and osteopontin were markers of proinflammatory gene products. p-ERK, p-p38, and NF-κB served as markers of proinflammatory cell signaling.

Multiple 6-μm-thick frozen sections cut from OCT compound-embedded frozen materials were postfixed for 10 min at 4°C in 100% acetone, rinsed in 150 mM phosphate-buffered saline, pH 7.6 (PBS), quenched for 10 min with 3% H_2O_2, rinsed in PBS, treated for 20 min at room temperature with 3% BSA or 3% skim milk in PBS, processed with the Avidin/Biotin blocking kit (Vector Laboratories, Burlingame, CA, USA) according to the manufacturer's instructions, and then incubated overnight at 4°C with the primary antibodies. Immunoreaction was visualized by the avidin-biotin-immunoperoxidase complex (ABC) method using the appropriate Vectastain ABC kits (Vector) according to the manufacturer's instructions. The chromogen was 3,3'-diaminobenzidine hydrochloride (DAB), and the counterstain was hematoxylin. Negative reaction control sections were obtained by omission of the primary antibodies or by incubating with nonimmune IgG derived from the same animal species as those producing the antibodies. Immunostained sections were observed with a light microscope (Olympus, Tokyo, Japan), and immunohistochemical localization of p-cSrc was identified by comparison with consecutive sections stained with H&E and immunostained for CD68, SMA, OxPC, tissue factor, osteopontin, p-ERK, p-p38, and NF-κB. In addition, immunohistochemical localization of p-cSrc was strictly verified by comparison with that of p-p38 and NF-κB using the double immunostaining method. Briefly, sections were incubated with the rabbit anti-p-p38 antibody or the goat anti-NF-κB antibody, and immunoreaction was detected by the ABC method with DAB as the chromogen. After photomicrographing immunoreactive structures, the immunostained sections were then incubated with the mouse anti-p-cSrc antibody, and immunoreaction was detected by the polymer-immunocomplex method using the Envision system kit (DakoCytomation) with NiCl$_2$/DAB as the chromogen. The location of the p-cSrc determinants (blue) was compared with the initially taken photographs of the p-p38 and NF-κB determinants (brown). Thus, appearance of 'dark blue stain' was considered as the colocalization of the blue pigments with the brown pigments.

Image analysis

To quantify macrophage content in CAS lesions, the proportion of CD68-immunoreactive area in each plaque was measured by image analysis. In brief, sections immunostained for CD68 were observed by light microscopy, and

the photogenic data were digitally imported into a personal computer using Photoshop image software. Both the CD68-immunoreactive area (mm^2) and the total area (mm^2) in a plaque were measured using NIH image software.

Statistics

The relationship between macrophage content and cSrc activation in the examined cases was statistically verified by nonparametric correlation analysis. Macrophage content in each plaque was expressed as a percentage of the CD68-immunoreactive area in the total area on a section. cSrc activation in each plaque was expressed as a relative value of the densitometric p-cSrc/β-actin ratio on a lane. Linear equation (y=ax+b) and correlation coefficient (r) were obtained, and r value more than 0.6 was considered to be strongly correlated. The examined lesions were then divided into macrophage-rich plaques (MRPs) and macrophage-poor plaques (MPPs), as described previously [23]; MRPs and MPPs were defined as having macrophage content more than 5% and less than 5%, respectively. The densitometric p-cSrc/β-actin data in the MRP and MPP groups were expressed as mean±standard deviation, and compared by unpaired Student's t-test between the two groups. The histopathological findings were compared by using chi square test between the two groups. P value less than 0.05 was considered statistically significant.

III. Results

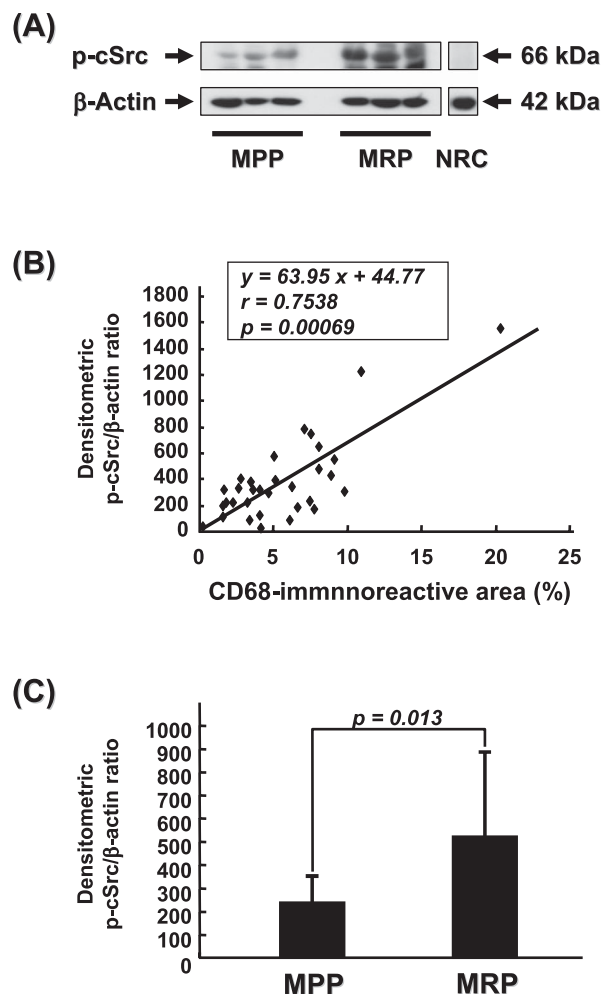### Relationship between macrophage content and cSrc activation

Immunoreactive signals for p-cSrc and β-actin appeared on immunoblots at 66 kDa and 42 kDa, respectively (Fig. 1A). No immunoreaction product was detectable on negative reaction control lanes. There was a strong positive correlation between the CD68-immunoreactive areas on sections and the optical p-cSrc densities on blots (Fig. 1B). The 32 examined cases were divided into 14 MPP cases and 18 MRP cases. Unpaired Student's t-test revealed that the optical p-cSrc densities on blots were significantly increased in the MRP group compared to the MPP group (Fig. 1C).

Comparison of histopathological findings between the MPP and MRP groups

The histopathological findings were compared by chi square test between the MRP and MPP groups (Table 2). Based on the hallmarks of plaque instability, the occurrence of plaque hemorrhage and thrombus formation significantly increased in the MRP group than in the MPP group. By contrast, there was no significant difference in the occurrence of ulceration and calcification of the CAS plaques between the two groups.

Immunohistochemical observations of p-cSrc and related substances

No immunoreaction product deposit was visible on negative reaction control sections (data not shown). At a low
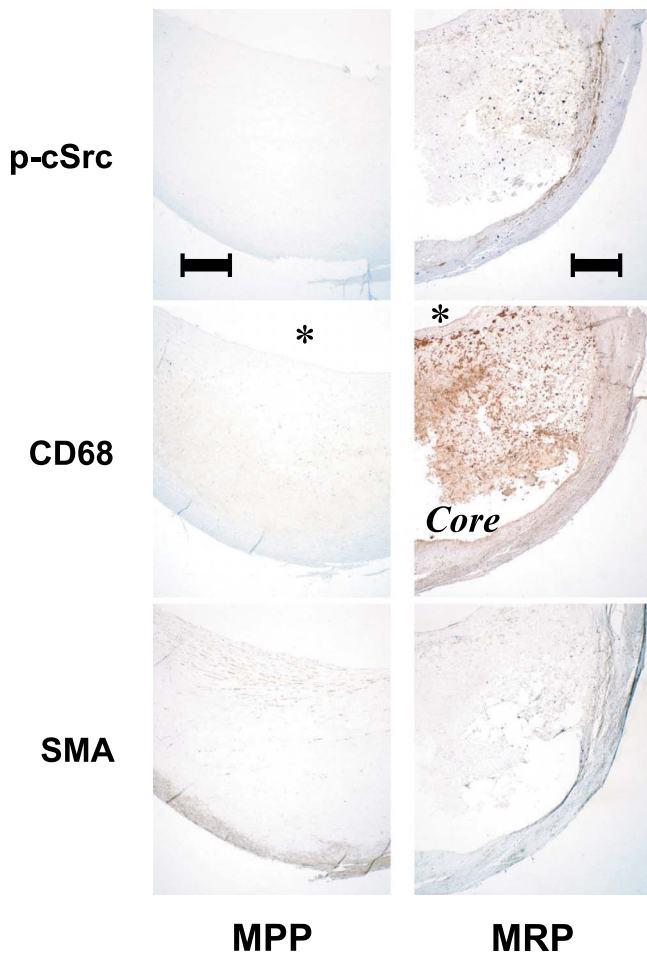

Fig. 1. Quantitative measurements of p-cSrc in CEA specimens. (**A**) Representative results of immunoblotting of p-cSrc and β-actin detected by the chemiluminescence method. (**B**) Correlation between macrophage content and cSrc activation. (**C**) Comparison of cSrc activation levels between the MPP and MRP groups. CEA, carotid endarterectomy; MPP, macrophage-poor plaque; MRP, macrophage-rich plaque; NRC, negative reaction control; p-cSrc, active form of cSrc phosphorylated at Y^{416}.

Table 2. *Comparison of histopathological features between the two groups*

Characteristics	MPP group (cases)	MRP group (cases)	P value
Number of subjects	14	18	
Plaque morphology			
Ulceration	2	3	NS
Hemorrhage	3	13	0.011
Thrombus formation	0	9	0.0018
Calcification	12	16	NS

MPP, macrophage-poor plaque; MRP, macrophage-rich plaque; NS, not significant.

Fig. 2. Loupe findings of consecutive MPP and MRP sections immunostained for p-cSrc, CD68, and SMA. Immunoreaction on all sections is visualized by the ABC method with DAB as the chromogen (brown). Bar=1 mm. ABC, avidin-biotin-immunoperoxidase complex; DAB, 3,3'-diaminobenzidine tetrahydrochloride; MPP, macrophage-poor plaque; MRP, macrophage-rich plaque; p-cSrc, active form of cSrc phosphorylated at Y^{416}; SMA, α-smooth muscle actin.
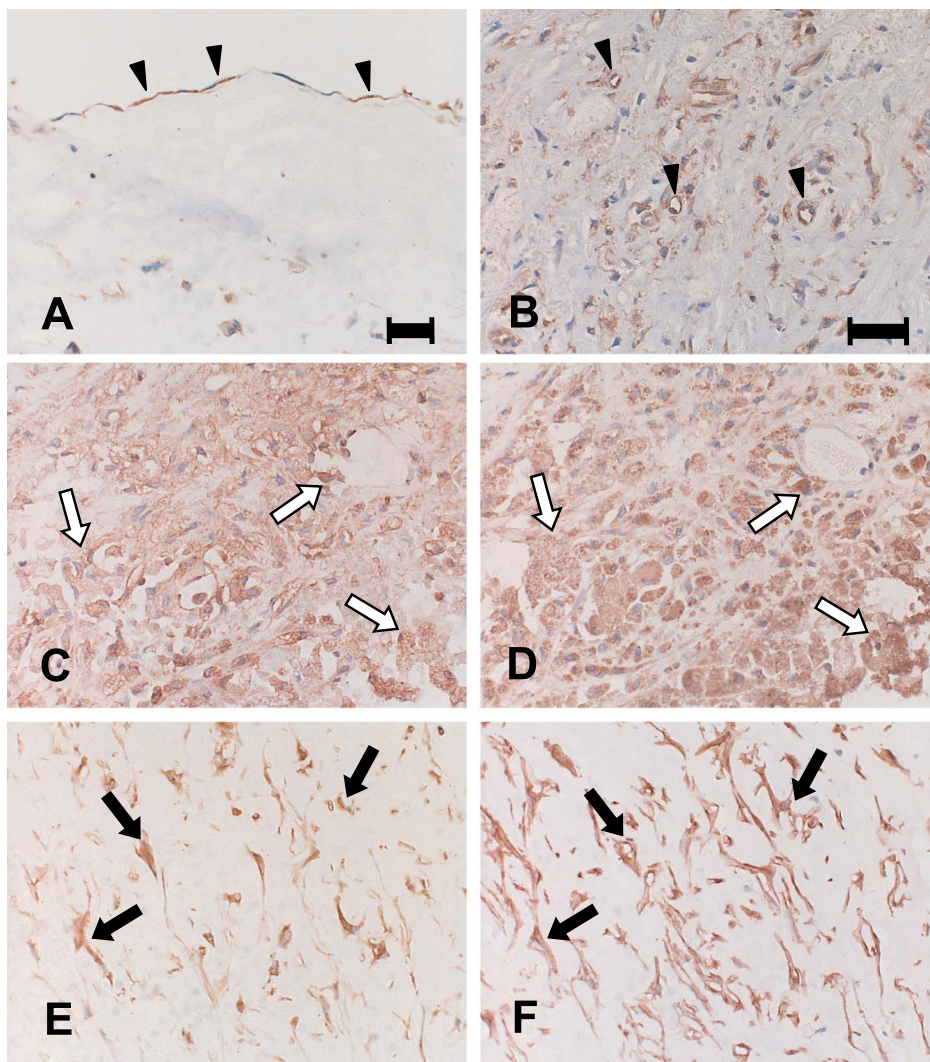
IV. Discussion

In the present study, it is noteworthy that p-cSrc was detected in human CAS lesions. There was a strong positive correlation between the CD68-immunoreactive areas on sections and the p-cSrc-immunoreactive densities on blots. This suggests that cSrc activation is enhanced in parallel with an increase in macrophage content in atherosclerotic lesions. The fact that both plaque hemorrhage and thrombus formation as the histopathological hallmarks of plaque instability were more common in the MRP group than in the MPP group shows the close relevance between macrophage content and plaque destabilization, as previously discussed [16]. The lack of difference in the occurrence of calcification between the two groups suggests dual roles for osteopontin in atherogenesis, including plaque inflammation and extracellular calcification. Furthermore, p-cSrc immunoreactivity was localized in VECs, macrophages, and VSMCs in CAS plaques. Several experimental studies have indicated that macrophage content in atherosclerotic lesions reflects inflammatory activity and plaque instability [11, 24, 32, 36, 37]. Given these observations, cSrc activation in lesional cells may be involved in inflammation and instability of atherosclerotic lesions.

Some *in vitro* studies have demonstrated that the binding of OxLDL, FVIIa, and osteopontin to their specific receptors gives rise to cSrc activation, resulting in the activation of inflammatory cell signaling [17, 24, 35]. In relation to this, we demonstrated the colocalization of p-cSrc with OxLDL, tissue factor, and osteopontin in lesional cells such as VECs, macrophages, and VSMCs. After uptake into the lesional cells via scavenger receptors, OxLDL in the cytoplasm activates cSrc [9, 17, 20]. It is known that inflamed plaques have greater levels of the hepatocyte-produced, plasma-mediated FVIIa, as a result of increased endothelial permeability in the lesions. This leads to increased chances of FVIIa binding to the receptor tissue factor, resulting in cSrc activation [8, 26–28, 35]. Similarly, osteopontin binding to the receptor integrin $\alpha_V\beta_3$, CD44 or fibronectin induces cSrc activation [24]. In addition, the binding of angiotensin II, one of the most important factors involved in atherogenesis, to AT_1R also brings about cSrc activation [3, 21, 30]. These studies attributed cSrc activation to increased oxidative stress and cytosolic calcium levels.

It has been shown that cSrc activation exerts critical effects on the induction of proinflammatory gene products via activation of the MAPK pathway and the NF-κB pathway [3–5, 7, 8, 15, 21, 26, 27, 35, 38]. In relation to this, we demonstrated the colocalization of p-cSrc with p-ERK, p-p38, and NF-κB in CAS lesions, as previously described [19, 21, 22, 25, 31]. Several experimental studies have shown that activated cSrc catalyzes the phosphorylation of phosphatidyl inositol 3-kinase (PI3K) and protein kinase C (PKC) [4, 5, 7, 8, 15, 26, 27, 35] to activate them. PI3K activates ERK and p38 via activation of Ras and Rac1, respectively, while PKC activates ERK and NF-κB via activation of Raf-1 and inhibitor of κB kinase, respectively. Alternatively, both the

magnification, p-cSrc immunoreactivity was distributed in the CAS plaques (Fig. 2), and seemed to increase in the MRP group compared with the MPP group. The distribution of p-cSrc appeared to overlap with that of CD68 and SMA to some extent; however, the cSrc immunoreactivity was less intense in large foamy macrophages neighboring the lipid core. At a higher magnification, p-cSrc immunoreactivity was localized in the cytoplasm of VECs lining the inner surface of carotid arteries and newly formed capillary vessels in atherosclerotic lesions as well as macrophages and migrating VSMCs (Fig. 3). p-cSrc immunoreactivity in the cytoplasm of these lesional cells was colocalized with OxPC, tissue factor, osteopontin, p-ERK, p-p38, and NF-κB (Fig. 4). NF-κB immunoreactivity was also localized in the nucleus of the lesional cells.

Fig. 3. Photomicrographs of MRP sections immunostained for p-cSrc (**A–C, E**), CD68 (**D**) and SMA (**F**). Sections (**C, E**) are consecutive to sections (**D, F**), respectively. Immunoreaction on all sections is visualized by the ABC method with DAB as the chromogen (brown). Arrowheads, blank arrows, and solid arrows indicate VECs, macrophages, and VSMCs, respectively. Bar=50 μm (**A–F**). ABC, avidin-biotin-immunoperoxidase complex; DAB, 3,3'-diaminobenzidine tetrahydrochloride; MRP, macrophage-rich plaque; p-cSrc, active form of cSrc phosphorylated at Y^{416}; SMA, α-smooth muscle actin; VECs, vascular endothelial cells; VSMCs, vascular smooth muscle cells.

MAPK and NF-κB pathways induce tissue factor [2, 18, 22] and osteopontin [38], which have been shown to be overexpressed in symptomatic CAS plaques [10, 14]. Moreover, both the binding of FVIIa and osteopontin to their specific receptors, as mentioned above, consequently induce cSrc activation again. Thus, it is likely that cSrc activation may contribute to persistent inflammation in CAS lesions.

Collectively, we demonstrated the following four findings using CEA specimens: (1) the strong positive correlation between macrophage content and cSrc activation, (2) the increased vulnerability of MRPs compared to MPPs, (3) the localization of p-cSrc in VECs, macrophages, and VSMCs, and (4) the colocalization of p-cSrc with the upstream OxLDL, tissue factor, and osteopontin and the downstream activated ERK, p38, and NF-κB. Our results suggest that cSrc activation in lesional cells mediates persistent inflammation in CAS plaques and contributes to plaque destabilization, and point to the possibility that the inhibition of cSrc may ameliorate these pathological conditions. Recent investigations have documented implications for cSrc activation in transactivation and nuclear translocation of the transcription factor signal transducer and activator of transcription (STAT) in atherosclerosis models [21, 39]. Little is known, however, about the relationship between cSrc and STAT in atherogenesis. Answers to this and other questions concerning the modulation of cSrc activity need to be addressed to further the understanding of the pathomechanism of plaque destabilization and the prevention of ischemic events in the brain.
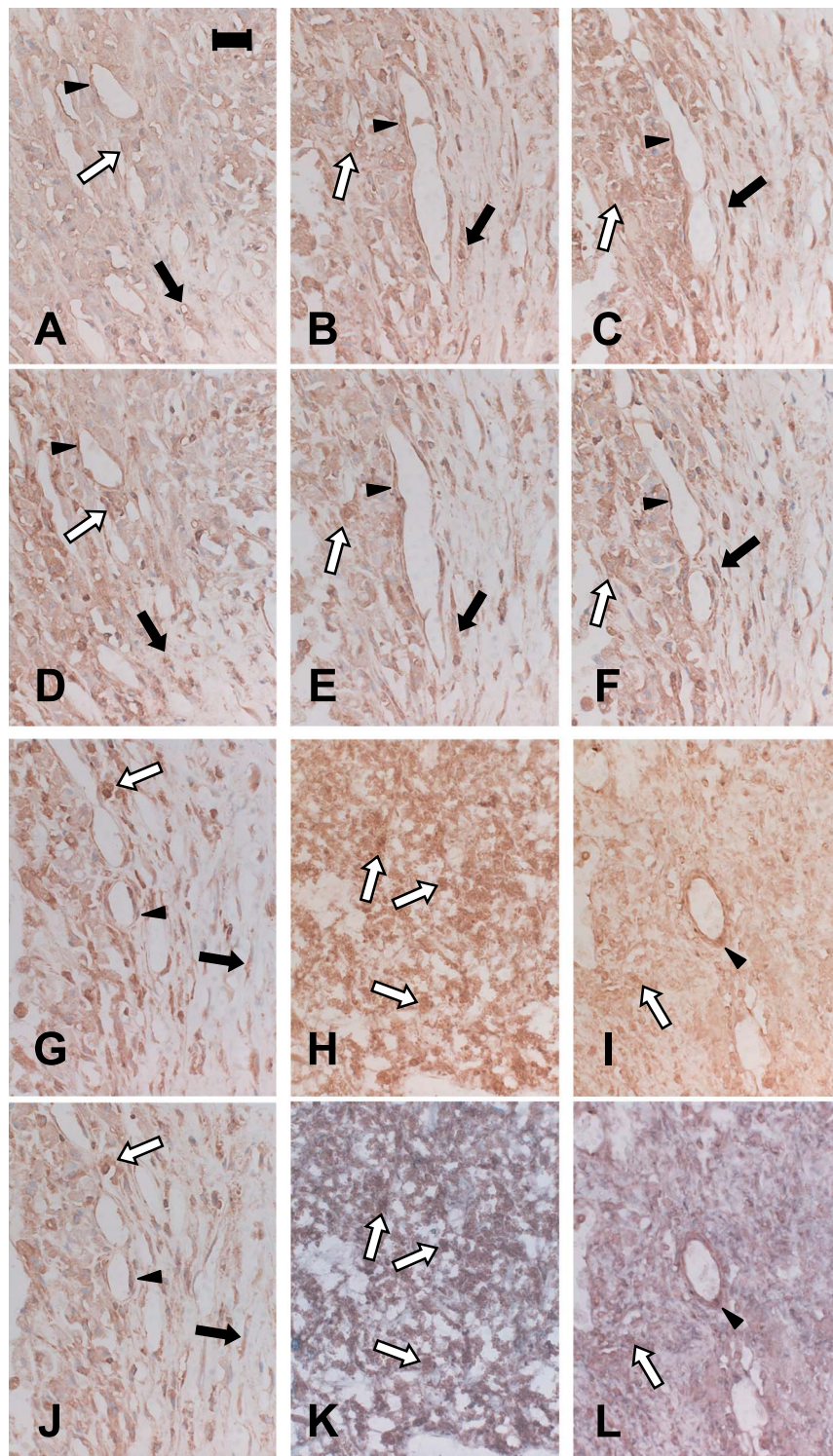
Fig. 4. Photomicrographs of MRP sections immunostained for p-cSrc (**D–F, J–L**), OxPC (**A**), tissue factor (**B**), osteopontin (**C**), p-ERK (**G**), p-p38 (**H**), and NF-κB (**I**). Panels (**A–C, G**) indicate identical regions to panels (**D–F, H**), respectively, on consecutive sections. Panels (**H, I**) indicate identical regions to panels (**K, L**), respectively, on the same sections. Immunoreaction on all sections is visualized by the ABC method with DAB as the chromogen (brown) (**A–L**), and in addition, panels (**K, L**) show double immunostaining for p-cSrc on panels (**H, I**), respectively, by the PIC method with DAB/NiCl$_2$ as the chromogen (blue & brown). Arrowheads, blank arrows, and solid arrows indicate VECs, macrophages, and VSMCs, respectively. Bar=50 μm (**A–L**). ABC, avidin-biotin-immunoperoxidase complex; DAB, 3,3'-diaminobenzidine tetrahydrochloride; MRP, macrophage-rich plaque; NF-κB, nuclear factor-κB; OxPC, oxidized phosphatidylcholine; p-cSrc, active form of cSrc phosphorylated at Y[416]; p-ERK, active form of extracellular signal-regulated kinase phosphorylated at Y[204]; PIC, polymer-immunocomplex; p-p38, active form of p38 mitogen-activated protein kinase phosphorylated at Y[182].

VI.   References

1. Adams, H. P., Del Zoppo, G., Alberts, M. J., Bhatt, D. L., Brass, L., Furlan, A., Grubb, R. L., Higashida, R. T., Jauch, E. C., Kidwell, C., Lyden, P. D., Morgenstern, L. B., Qureshi, A. I., Rosenwasser, R. H., Scott, P. A. and Wijdicks, E. F. M. (2007) Guidelines for early management of adults with ischemic stroke: a guideline from the American Heart Association/American Stroke Association Stroke Council, Clinical Cardiology Council, Cardiovascular Radiology and Intervention Council, and the Atherosclerotic Peripheral Vascular Disease and Quality of Care Outcomes in Research Interdisciplinary Working Groups: the American Academy of Neurology affirms the value of this guideline as an educational tool for neurologists. *Stroke* 38; 1655–1711.

2. Bohgaki, N., Atsumi, T., Yamashita, Y., Yasuda, S., Sakai, Y., Furusaki, A., Bohgaki, T., Amengual, O., Amasaki, Y. and Koike, T. (2004) The p38 mitogen-activated protein kinase (MAPK) pathway mediates induction of the tissue factor gene in monocytes stimulated with human monoclonal anti-β_2 glycoprotein I antibodies. *Int. Immunol.* 16; 1633–1641.

3. Bokemeyer, D., Schmitz, U. and Kramer, H. J. (2000) Angiotensin II-induced growth of vascular smooth muscle cells requires an Src-dependent activation of the epidermal growth factor receptor. *Kid. Int.* 58; 549–558.

4. Bouchard, V., Demers, M. J., Thibodeau, S., Laquerre, V., Fujita, N., Tsuruo, T., Beaulieu, J. F., Gauthier, R., Vézina, A., Villeneuve, L. and Vachon, P. H. (2007) Fak/Src signaling in human intestinal epithelial cell survival and anoikis: differentiation state-specific uncoupling with the PI3-K/Akt-1 and MEK/Erk pathways. *J. Cell. Physiol.* 212; 717–728.

5. Chang, Y. J., Wu, M. S., Lin, J. T., Sheu, B. S., Muta, T., Inoue, H. and Chen, C.-C. (2004) Induction of cyclooxygenase-2 overexpression in human gastric epithelial cells by *Helicobacter pylori* involves TLR2/TLR9 and c-Src dependent nuclear factor-κB activation. *Mol. Pharmacol.* 66; 1465–1477.

6. Chiba, S., Okamoto, H., Kon, S., Kimura, C., Murakami, M., Inobe, M., Matsui, Y., Sugawara, T., Shimizu, T., Ueda, T. and Kitabatake, A. (2002) Development of atherosclerosis in osteopontin transgenic mice. *Heart Vessels* 16; 111–117.

7. Cho, H.-M., Choi, S. H., Hwang, K.-C., Oh, S.-Y., Kim, H.-G., Yoon, D.-H., Choi, M.-A., Lim, S., Song, Y., Jang, Y. and Kim, T. W. (2005) The Src/PLC/PKC/MEK/ERK signaling pathway is involved in aortic smooth muscle cell proliferation induced by glycated LDL. *Mol. Cells* 19; 60–66.

8. Cirillo, P., Calì, G., Golino, P., Calabrò, P., Forte, L., De Rosa, S., Pacileo, M., Ragni, M., Scopacasa, F., Nitsch, L. and Chiariello, M. (2004) Tissue factor binding of activated factor VII triggers smooth muscle cell proliferation via extracellular signal-regulated kinase activation. *Circulation* 109; 2911–2916.

9. Foncea, R., Carvajal, C., Almarza, C. and Leighton, F. (2000) Endothelial cell oxidative stress and signal transduction. *Biol. Res.* 33; 89–96.

10. Golledge, J., McCann, M., Mangan, S., Lam, A. and Karan, M. (2004) Osteoprotegerin and osteopontin are expressed at high concentrations within symptomatic carotid atherosclerosis. *Stroke* 35; 1636–1641.

11. Hansson, G. K. (2005) Inflammation, atheroslecrosis, and coronary artery disease. *N. Engl. J. Med.* 352; 1685–1695.

12. Hasenstab, D., Lea, H., Hart, C. E., Lok, S. and Clowes, A. W. (2000) Tissue factor overexpression in rat arterial neointima models thrombosis and progression of advanced atherosclerosis. *Circulation* 101; 2651–2657.

13. Itabe, H., Takeshima, E., Iwasaki, H., Kimura, J., Yoshida, Y., Imanaka, T. and Takano, T. (1994) A monoclonal antibody against oxidized lipoprotein recognizes foam cells in atherosclerotic lesions. *J. Biol. Chem.* 269; 15274–15279.

14. Jander, S., Sitzer, M., Wendt, A., Schroeter, M., Buchkremer, M., Siebler, M., Müller, W., Sandmann, W. and Stoll, G. (2001) Expression of tissue factor in high-grade carotid artery stenosis. Association with plaque destabilization. *Stroke* 32; 850–854.

15. Kanda, Y. and Watanabe, Y. (2005) Thrombin-induced glucose transport via Src-p38 MAPK pathway in vascular smooth muscle cells. *Br. J. Pharmacol.* 146; 60–67.

16. Lee, R. T. and Libby, P. (1997) The unstable atheroma. *Arterioscler. Thromb. Vasc. Biol.* 17; 1859–1867.

17. Leonarduzzi, G., Arkan, M. C., Başağa, H., Chiarpotto, E., Sevenian, A. and Poli, G. (2000) Lipid oxidation products in cell signaling. *Free Radic. Biol. Med.* 28; 1370–1378.

18. López-Pedrera, C., Buendía, P., Cuadrado, M. J., Siendones, E., Aguirre, M. A., Barbarroja, N., Montiel-Duarte, C., Torres, A., Khamashta, M. and Velasco, F. (2006) Antiphospholipid antibodies from patients with the antiphospholipid syndrome induce monocyte tissue factor expression through the simultaneous activation of NF-κB/Rel proteins via the p38 mitogen-activated protein kinase pathway, and of the MEK-1/ERK pathway. *Arthritis Rheum.* 54; 301–311.

19. Martin-Ventura, J. L., Blanco-Colio, L. M., Muñoz-Garcia, B., Gómez-Hernández, A., Arribas, A., Ortega, L., Tuñon, J. and Egido, J. (2004) NF-κB activation and Fas ligand overexpression in blood and plaques of patients with carotid atherosclerosis. Potential implication in plaque instability. *Stroke* 35; 458–463.

20. Maschberger, P., Bauer, M., Baumann-Siemons, J., Zangl, K. J., Negrescu, E. V., Reininger, A. J. and Siess, W. (2000) Mildly oxidized low density lipoprotein rapidly stimulates via activation of the lysophosphatidic acid receptor Src family and Syk tyrosine kinases and Ca^{2+} influx in human platelets. *J. Biol. Chem.* 275; 19159–19166.

21. Mheta, P. K. and Griendling, K. K. (2007) Angiotensin II cell signaling: physiological and pathological effects in the cardiovascular system. *Am. J. Physiol. Cell Physiol.* 292; C82–C97.

22. Monaco, C., Andreakos, E., Kiriakidis, S., Mauri, C., Bicknell, C., Foxwell, B., Cheshire, N., Paleolog, E. and Feldmann, M. (2004) Canonical pathway of nuclear factor κB activation selectively regulates proinflammatory and prothrombotic responses in human atherosclerosis. *Proc. Natl. Acad. Sci. U S A* 101; 5634–5639.

23. Nishi, K., Itabe, H., Uno, M., Kitazato, K. T., Horiguchi, H., Shinno, K. and Nagahiro, S. (2002) Oxidized LDL in carotid plaques and plasma associates with plaque instability. *Arterioscler. Thromb. Vasc. Biol.* 22; 1649–1654.

24. Ohsuzu, F. (2004) The roles of cytokines, inflammation and immunity in vascular diseases. *J. Atheroscler. Thromb.* 11; 313–321.

25. Omura, T., Yoshiyama, M., Izumi, Y., Kim, S., Matsumoto, R., Enomoto, S., Kusuyama, T., Nishuya, D., Nakamura, Y., Akioka, K., Iwao, H., Takeuchi, K. and Yoshikawa, J. (2005) Involvement of c-Jun NH$_2$ terminal kinase and p38MAPK in rapamycin-mediated inhibition of neointimal formation in rat carotid arteries. *J. Cardiovasc. Pharmacol.* 46; 519–525.

26. Ott, I., Weigand, B., Michl, R., Seitz, I., Sabbari-Erfani, N., Neumann, F. J. and Schömig, A. (2005) Tissue factor cytoplasmic domain stimulates migration by activation of the GTPase Rac1 and the mitogen-activated protein kinase p38. *Circulation* 111; 349–355.

27. Poulsen, L. K., Jacobsen, N., Sørensen, B. B., Bergenhem, N. C. H., Kelly, J. D., Foster, D. C., Thastrup, O., Ezban, M. and Petersen, L. C. (1998) Signal transduction via the mitogen-activated protein kinase pathway induced by binding of coagulation factor VIIa to tissue factor. *J. Biol. Chem.* 273; 6228–6232.

28. Price, G. C., Thompson, S. A. and Kam, P. C. A. (2004) Tissue factor and tissue factor pathway inhibitor. *Anaesthesia* 59; 483–492.

29. Sapan, C. V., Lundblad, R. L. and Price, N. C. (1999) Colorimetric protein assay techniques. *Biotechnol. Appl. Biochem.* 29; 99–108.

30. Seshiah, P. N., Weber, D. S., Rocic, P., Valppu, L., Taniyama, Y. and Griendling, K. K. (2002) Angiotensin II stimulation of NAD(P)H oxidase activity. Upstream mediators. *Circ. Res.* 91; 406–413.

31. Squadrito, F., Minutoli, L., Esposito, M., Bitto, A., Marini, H., Seminara, P., Crisafuli, A., Passaniti, M., Adamo, E. B., Marini, R., Guarini, S. and Altavilla, D. (2005) Lipid peroxidation triggers both c-Jun N-terminal kinase (JNK) and extracellular-regulated kinase (ERK) activation and neointimal hyperplasia induced by cessation of blood flow in the mouse carotid artery. *Atherosclerosis* 178; 295–302.

32. Stoll, G. and Bendszus, M. (2006) Inflammation and atherosclerosis. Novel insights into plaque formation and destabilization. *Stroke* 37; 1923–1932.

33. Ström, Å., Franzén, A., Wännerud, C., Knutsson, A.-K., Heinegård, D. and Hultgårdh-Nilsson, A. (2004) Altered vascular remodeling in osteopontin-deficient atherosclerotic mice. *J. Vasc. Res.* 41; 314–322.

34. Tilley, R. E., Pedersen, B., Pawlinski, R., Sato, Y., Erlich, J. H., Shen, Y., Day, S., Huang, Y., Eitzman, D. T., Boisvert, W. A., Curtiss, L. K., Fay, W. P. and Mackman, N. (2006) Atherosclerosis in mice is not affected by a reduction in tissue factor expression. *Arterioscler. Thromb. Vasc. Biol.* 26; 555–562.

35. Versteeg, H. H., Hoedemaeker, I., Diks, S. H., Stam, J. C., Spaargaren, M., Van Bergen En Henegouen, P. M. P., Van Deventer, S. J. H. and Peppelenbosch, M. P. (2000) Factor VIIa/tissue factor-induced signaling via activation of Src-like kinases, phosphatidylinositol 3-kinase, and Rac. *J. Biol. Chem.* 275; 28750–28756.

36. Viles-Gonzalez, J. F., Anand, S. X., Valdiviezo, C., Zafar, M. U., Hutter, R., Sanz, J., Rius, T., Poon, M., Fuster, V. and Badimon, J. J. (2004) Update in atherothrombotic disease. *Mount Sainai J. Med.* 71; 197–208.

37. Virmani, R., Ladich, E. R., Burke, A. P. and Kolodgie, F. D. (2006) Histopathology of carotid atherosclerotic disease. *Neurosurgery* 59 (Suppl); S3-219–S3-229.

38. Xie, Z., Pimental, D. R., Lohan, S., Vasertriger, A., Pligavko, C., Colucci, W. S. and Singh, K. (2001) Regulation of angiotensin II-stimulated osteopontin expression in cardiac microvascular endothelial cells: role of p42/44 mitogen-activated protein kinase and reactive oxygen species. *J. Cell Physiol.* 188; 132–138.

39. Yeh, M., Gharavi, N. M., Choi, J., Hsieh, X., Reed, E., Mouillesseaux, K. P., Cole, A. L., Reddy, S. T. and Berliner, J. A. (2004) Oxidized phospholipids increase interleukin 8 (IL-8) synthesis by activation of the c-src/signal transducers and activators of transcription (STAT) 3 pathway. *J. Biol. Chem.* 279; 30175–30181.